

Search for the Decay $B_s^0 \rightarrow \eta'\eta$

N. K. Nisar,³ V. Savinov,⁷² I. Adachi,^{19,15} H. Aihara,⁹⁰ S. Al Said,^{83,39} D. M. Asner,³ H. Atmacan,⁷ T. Aushev,²¹ R. Ayad,⁸³ V. Babu,⁸ S. Bahinipati,²⁵ P. Behera,²⁸ J. Bennett,⁵³ M. Bessner,¹⁸ V. Bhardwaj,²⁴ B. Bhuyan,²⁶ T. Bilka,⁵ J. Biswal,³⁶ G. Bonvicini,⁹⁵ A. Bozek,⁶³ M. Bračko,^{50,36} T. E. Browder,¹⁸ M. Campajola,^{33,58} D. Červenkov,⁵ M.-C. Chang,¹⁰ V. Chekelian,⁵¹ A. Chen,⁶⁰ B. G. Cheon,¹⁷ K. Chilikin,⁴⁵ H. E. Cho,¹⁷ K. Cho,⁴¹ S.-K. Choi,¹⁶ Y. Choi,⁸¹ S. Choudhury,²⁷ D. Cinabro,⁹⁵ S. Cunliffe,⁸ S. Das,⁴⁹ N. Dash,²⁸ G. De Nardo,^{33,58} R. Dhamija,²⁷ F. Di Capua,^{33,58} Z. Doležal,⁵ T. V. Dong,¹¹ S. Dubey,¹⁸ S. Eidelman,^{4,67,45} D. Epifanov,^{4,67} T. Ferber,⁸ D. Ferlewicz,⁵² A. Frey,¹⁴ B. G. Fulsom,⁶⁹ R. Garg,⁷⁰ V. Gaur,⁹⁴ N. Gabyshev,^{4,67} A. Garmash,^{4,67} A. Giri,²⁷ P. Goldenzweig,³⁷ Y. Guan,⁷ K. Gudkova,^{4,67} C. Hadjivasiliou,⁶⁹ S. Halder,⁸⁴ T. Hara,^{19,15} O. Hartbrich,¹⁸ K. Hayasaka,⁶⁵ H. Hayashii,⁵⁹ M. T. Hedges,¹⁸ C.-L. Hsu,⁸² T. Iijima,^{57,56} K. Inami,⁵⁶ A. Ishikawa,^{19,15} R. Itoh,^{19,15} M. Iwasaki,⁶⁸ Y. Iwasaki,¹⁹ W. W. Jacobs,²⁹ S. Jia,¹¹ Y. Jin,⁹⁰ C. W. Joo,³⁸ K. K. Joo,⁶ J. Kahn,³⁷ A. B. Kaliyar,⁸⁴ K. H. Kang,⁴³ G. Karyan,⁸ T. Kawasaki,⁴⁰ H. Kichimi,¹⁹ C. Kiesling,⁵¹ C. H. Kim,¹⁷ D. Y. Kim,⁸⁰ S. H. Kim,⁷⁷ Y.-K. Kim,⁹⁷ K. Kinoshita,⁷ P. Kodyš,⁵ T. Konno,⁴⁰ A. Korobov,^{4,67} S. Korpar,^{50,36} E. Kovalenko,^{4,67} P. Križan,^{46,36} R. Kroeger,⁵³ P. Krokovny,^{4,67} T. Kuhr,⁴⁷ M. Kumar,⁴⁹ R. Kumar,⁷³ K. Kumara,⁹⁵ A. Kuzmin,^{4,67} Y.-J. Kwon,⁹⁷ K. Lalwani,⁴⁹ J. S. Lange,¹² S. C. Lee,⁴³ Y. B. Li,⁷¹ L. Li Gioi,⁵¹ J. Libby,²⁸ K. Lieret,⁴⁷ D. Liventsev,^{95,19} C. MacQueen,⁵² M. Masuda,^{89,74} T. Matsuda,⁵⁴ D. Matvienko,^{4,67,45} M. Merola,^{33,58} F. Metzner,³⁷ R. Mizuk,^{45,21} G. B. Mohanty,⁸⁴ S. Mohanty,^{84,93} M. Nakao,^{19,15} A. Natochii,¹⁸ L. Nayak,²⁷ M. Nayak,⁸⁶ S. Nishida,^{19,15} K. Nishimura,¹⁸ S. Ogawa,⁸⁷ H. Ono,^{64,65} Y. Onuki,⁹⁰ P. Oskin,⁴⁵ P. Pakhlov,^{45,55} G. Pakhlova,^{21,45} T. Pang,⁷² S. Pardi,³³ H. Park,⁴³ S.-H. Park,¹⁹ S. Patra,²⁴ S. Paul,^{85,51} T. K. Pedlar,⁴⁸ R. Pestotnik,³⁶ L. E. Pilonen,⁹⁴ T. Podobnik,^{46,36} E. Prencipe,²² M. T. Prim,² M. Röhrken,⁸ A. Rostomyan,⁸ N. Rout,²⁸ G. Russo,⁵⁸ D. Sahoo,⁸⁴ S. Sandilya,²⁷ A. Sangal,⁷ L. Santelj,^{46,36} T. Sanuki,⁸⁸ G. Schnell,^{1,23} J. Schueler,¹⁸ C. Schwanda,³¹ Y. Seino,⁶⁵ K. Senyo,⁹⁶ M. E. Sevir,⁵² M. Shapkin,³² C. Sharma,⁴⁹ C. P. Shen,¹¹ J.-G. Shiu,⁶² B. Shwartz,^{4,67} F. Simon,⁵¹ E. Solovieva,⁴⁵ S. Stanič,⁶⁶ M. Starič,³⁶ Z. S. Stottler,⁹⁴ M. Sumihama,¹³ T. Sumiyoshi,⁹² M. Takizawa,^{78,20,75} U. Tamponi,³⁴ K. Tanida,³⁵ F. Tenchini,⁸ K. Trabelsi,⁴⁴ M. Uchida,⁹¹ T. Uglov,^{45,21} Y. Unno,¹⁷ S. Uno,^{19,15} P. Urquijo,⁵² R. Van Tonder,² G. Varner,¹⁸ A. Vossen,⁹ E. Waheed,¹⁹ C. H. Wang,⁶¹ M.-Z. Wang,⁶² P. Wang,³⁰ X. L. Wang,¹¹ S. Watanuki,⁴⁴ E. Won,⁴² X. Xu,⁷⁹ B. D. Yabsley,⁸² W. Yan,⁷⁶ S. B. Yang,⁴² H. Ye,⁸ Z. P. Zhang,⁷⁶ V. Zhilich,^{4,67} and V. Zhukova⁴⁵

(The Belle Collaboration)

¹*Department of Physics, University of the Basque Country UPV/EHU, 48080 Bilbao*

²*University of Bonn, 53115 Bonn*

³*Brookhaven National Laboratory, Upton, New York 11973*

⁴*Budker Institute of Nuclear Physics SB RAS, Novosibirsk 630090*

⁵*Faculty of Mathematics and Physics, Charles University, 121 16 Prague*

⁶*Chonnam National University, Gwangju 61186*

⁷*University of Cincinnati, Cincinnati, Ohio 45221*

⁸*Deutsches Elektronen-Synchrotron, 22607 Hamburg*

⁹*Duke University, Durham, North Carolina 27708*

¹⁰*Department of Physics, Fu Jen Catholic University, Taipei 24205*

¹¹*Key Laboratory of Nuclear Physics and Ion-beam Application (MOE) and Institute of Modern Physics, Fudan University, Shanghai 200443*

¹²*Justus-Liebig-Universität Gießen, 35392 Gießen*

¹³*Gifu University, Gifu 501-1193*

¹⁴*II. Physikalisches Institut, Georg-August-Universität Göttingen, 37073 Göttingen*

¹⁵*SOKENDAI (The Graduate University for Advanced Studies), Hayama 240-0193*

¹⁶*Gyeongsang National University, Jinju 52828*

¹⁷*Department of Physics and Institute of Natural Sciences, Hanyang University, Seoul 04763*

¹⁸*University of Hawaii, Honolulu, Hawaii 96822*

¹⁹*High Energy Accelerator Research Organization (KEK), Tsukuba 305-0801*

²⁰*J-PARC Branch, KEK Theory Center, High Energy Accelerator Research Organization (KEK), Tsukuba 305-0801*

²¹*Higher School of Economics (HSE), Moscow 101000*

²²*Forschungszentrum Jülich, 52425 Jülich*

²³*IKERBASQUE, Basque Foundation for Science, 48013 Bilbao*

- ²⁴Indian Institute of Science Education and Research Mohali, SAS Nagar, 140306
- ²⁵Indian Institute of Technology Bhubaneswar, Satya Nagar 751007
- ²⁶Indian Institute of Technology Guwahati, Assam 781039
- ²⁷Indian Institute of Technology Hyderabad, Telangana 502285
- ²⁸Indian Institute of Technology Madras, Chennai 600036
- ²⁹Indiana University, Bloomington, Indiana 47408
- ³⁰Institute of High Energy Physics, Chinese Academy of Sciences, Beijing 100049
- ³¹Institute of High Energy Physics, Vienna 1050
- ³²Institute for High Energy Physics, Protvino 142281
- ³³INFN - Sezione di Napoli, 80126 Napoli
- ³⁴INFN - Sezione di Torino, 10125 Torino
- ³⁵Advanced Science Research Center, Japan Atomic Energy Agency, Naka 319-1195
- ³⁶J. Stefan Institute, 1000 Ljubljana
- ³⁷Institut für Experimentelle Teilchenphysik, Karlsruher Institut für Technologie, 76131 Karlsruhe
- ³⁸Kavli Institute for the Physics and Mathematics of the Universe (WPI), University of Tokyo, Kashiwa 277-8583
- ³⁹Department of Physics, Faculty of Science, King Abdulaziz University, Jeddah 21589
- ⁴⁰Kitasato University, Sagamihara 252-0373
- ⁴¹Korea Institute of Science and Technology Information, Daejeon 34141
- ⁴²Korea University, Seoul 02841
- ⁴³Kyungpook National University, Daegu 41566
- ⁴⁴Université Paris-Saclay, CNRS/IN2P3, IJCLab, 91405 Orsay
- ⁴⁵P.N. Lebedev Physical Institute of the Russian Academy of Sciences, Moscow 119991
- ⁴⁶Faculty of Mathematics and Physics, University of Ljubljana, 1000 Ljubljana
- ⁴⁷Ludwig Maximilians University, 80539 Munich
- ⁴⁸Luther College, Decorah, Iowa 52101
- ⁴⁹Malaviya National Institute of Technology Jaipur, Jaipur 302017
- ⁵⁰University of Maribor, 2000 Maribor
- ⁵¹Max-Planck-Institut für Physik, 80805 München
- ⁵²School of Physics, University of Melbourne, Victoria 3010
- ⁵³University of Mississippi, University, Mississippi 38677
- ⁵⁴University of Miyazaki, Miyazaki 889-2192
- ⁵⁵Moscow Physical Engineering Institute, Moscow 115409
- ⁵⁶Graduate School of Science, Nagoya University, Nagoya 464-8602
- ⁵⁷Kobayashi-Maskawa Institute, Nagoya University, Nagoya 464-8602
- ⁵⁸Università di Napoli Federico II, 80126 Napoli
- ⁵⁹Nara Women's University, Nara 630-8506
- ⁶⁰National Central University, Chung-li 32054
- ⁶¹National United University, Miao Li 36003
- ⁶²Department of Physics, National Taiwan University, Taipei 10617
- ⁶³H. Niewodniczanski Institute of Nuclear Physics, Krakow 31-342
- ⁶⁴Nippon Dental University, Niigata 951-8580
- ⁶⁵Niigata University, Niigata 950-2181
- ⁶⁶University of Nova Gorica, 5000 Nova Gorica
- ⁶⁷Novosibirsk State University, Novosibirsk 630090
- ⁶⁸Osaka City University, Osaka 558-8585
- ⁶⁹Pacific Northwest National Laboratory, Richland, Washington 99352
- ⁷⁰Panjab University, Chandigarh 160014
- ⁷¹Peking University, Beijing 100871
- ⁷²University of Pittsburgh, Pittsburgh, Pennsylvania 15260
- ⁷³Punjab Agricultural University, Ludhiana 141004
- ⁷⁴Research Center for Nuclear Physics, Osaka University, Osaka 567-0047
- ⁷⁵Meson Science Laboratory, Cluster for Pioneering Research, RIKEN, Saitama 351-0198
- ⁷⁶Department of Modern Physics and State Key Laboratory of Particle Detection and Electronics, University of Science and Technology of China, Hefei 230026
- ⁷⁷Seoul National University, Seoul 08826
- ⁷⁸Showa Pharmaceutical University, Tokyo 194-8543
- ⁷⁹Soochow University, Suzhou 215006
- ⁸⁰Soongsil University, Seoul 06978
- ⁸¹Sungkyunkwan University, Suwon 16419
- ⁸²School of Physics, University of Sydney, New South Wales 2006
- ⁸³Department of Physics, Faculty of Science, University of Tabuk, Tabuk 71451
- ⁸⁴Tata Institute of Fundamental Research, Mumbai 400005
- ⁸⁵Department of Physics, Technische Universität München, 85748 Garching
- ⁸⁶School of Physics and Astronomy, Tel Aviv University, Tel Aviv 69978

⁸⁷Toho University, Funabashi 274-8510

⁸⁸Department of Physics, Tohoku University, Sendai 980-8578

⁸⁹Earthquake Research Institute, University of Tokyo, Tokyo 113-0032

⁹⁰Department of Physics, University of Tokyo, Tokyo 113-0033

⁹¹Tokyo Institute of Technology, Tokyo 152-8550

⁹²Tokyo Metropolitan University, Tokyo 192-0397

⁹³Utkal University, Bhubaneswar 751004

⁹⁴Virginia Polytechnic Institute and State University, Blacksburg, Virginia 24061

⁹⁵Wayne State University, Detroit, Michigan 48202

⁹⁶Yamagata University, Yamagata 990-8560

⁹⁷Yonsei University, Seoul 03722

We report the results of the first search for the decay $B_s^0 \rightarrow \eta' \eta$ using 121.4 fb⁻¹ of data collected at the $\Upsilon(5S)$ resonance with the Belle detector at the KEKB asymmetric-energy e^+e^- collider. We observe no significant signal and set a 90% confidence-level upper limit of 6.5×10^{-5} on the branching fraction of this decay.

PACS numbers: 13.25.Hw, 14.40.Nd

The charmless hadronic decay $B_s^0 \rightarrow \eta' \eta$ is suppressed in the Standard Model (SM) and proceeds only through transitions sensitive to Beyond-the-Standard-Model (BSM) physics [1]. BSM scenarios, such as a fourth generation of fermions, supersymmetry with broken R-parity, and a two-Higgs doublet model with flavor-changing neutral currents, could affect the branching fraction and CP asymmetry of this decay [2]. The expected branching fraction for $B_s^0 \rightarrow \eta' \eta$ in the SM spans a range of $(2 - 4) \times 10^{-5}$ [3–7]. Once branching fractions for two-body decays $B_{d,s}^0 \rightarrow \eta \eta$, $\eta' \eta$, and $\eta' \eta'$ are measured, it would be possible to extract CP -violating parameters using a formalism based on $SU(3)/U(3)$ symmetry [3]. To achieve this goal, at least four of these six branching fractions need to be measured. Only the branching fraction for $B_s^0 \rightarrow \eta' \eta'$ has been measured so far [8].

In this Letter, we report the results of the first search for the decay $B_s^0 \rightarrow \eta' \eta$ using the full Belle data sample of 121.4 fb⁻¹ collected at the $\Upsilon(5S)$ resonance. The inclusion of the charge-conjugate decay mode is implied throughout. The Belle detector was a large-solid-angle magnetic spectrometer that operated at the KEKB asymmetric-energy e^+e^- collider [9]. The detector components relevant to our study include a tracking system comprising a silicon vertex detector (SVD) and a central drift chamber (CDC), a particle identification (PID) system that consists of a barrel-like arrangement of time-of-flight scintillation counters (TOF) and an array of aerogel threshold Cherenkov counters (ACC), and a CsI(Tl) crystal-based electromagnetic calorimeter (ECL). All these components were located inside a superconducting solenoid coil that provided a 1.5 T magnetic field. A detailed description of the Belle detector can be found elsewhere [10].

The $\Upsilon(5S)$ resonance decays into $B_s^{*0} \bar{B}_s^{*0}$, $B_s^{*0} \bar{B}_s^0$, and $B_s^0 \bar{B}_s^0$ pairs, where the relative fractions of the two former decays are $f_{B_s^{*0} \bar{B}_s^{*0}} = (87.0 \pm 1.7)\%$ and $f_{B_s^{*0} \bar{B}_s^0} = (7.3 \pm$

1.4)% [11], respectively. Signal B_s^0 mesons originate from the direct decays of $\Upsilon(5S)$ or from radiative decays of the excited vector state B_s^{*0} . The $\Upsilon(5S)$ production cross section is 340 ± 16 pb [11]. To present our nominal result for $\mathcal{B}(B_s^0 \rightarrow \eta' \eta)$ we use the world average value for the fraction of $B_s^{(*)0} \bar{B}_s^{(*)0}$ in $b\bar{b}$ events $f_s = 0.201 \pm 0.031$ [12], the data sample is therefore estimated to contain $(16.60 \pm 2.68) \times 10^6$ B_s^0 mesons. We also report the results for $f_s \times \mathcal{B}(B_s^0 \rightarrow \eta' \eta)$.

To maximize discovery potential of the analysis and to validate the signal extraction procedure, we use a sample of background Monte Carlo (MC) simulated events equivalent to six times the data statistics. In addition, to estimate the overall reconstruction efficiency we use a high-statistics signal MC sample, where the other $B_s^{(*)0}$ meson decays according to known branching fractions [12]. Both samples are used to develop a model implemented in the unbinned extended maximum-likelihood (ML) fit to data. The MC-based model is validated with a control sample of $B^0 \rightarrow \eta' K_S^0$ decays reconstructed from 711 fb⁻¹ of $\Upsilon(4S)$ data.

We reconstruct η candidates using pairs of electromagnetic showers not matched to the projections of charged tracks to the ECL and therefore identified as photons. We require that the reconstructed energies of these showers exceed 50 (100) MeV in the barrel (endcap) region of the ECL. The larger energy threshold for the endcaps is due to the larger beam-related background in these regions. To reject hadronic showers mimicking photons, the ratio of the energies deposited by a photon candidate in the (3×3) and (5×5) ECL crystal arrays centered on the crystal with the largest deposited energy is required to exceed 0.75. The reconstructed invariant mass of the η candidates is required to be $515 \leq M(\gamma\gamma) \leq 580$ MeV/ c^2 , which corresponds, approximately, to a $\pm 3\sigma$ Gaussian resolution window around the nominal η mass [12]. To suppress misreconstructed η candidates, the absolute value of the cosine of the helicity angle ($\cos\theta_{\text{hel}}$) is re-

quired to be less than 0.97, where θ_{hel} is the angle between the laboratory-frame directions of the photon and its presumed parent evaluated in the rest frame of the latter.

The η' candidates are formed by combining pairs of oppositely charged pions with the η candidates. We require the reconstructed η' invariant mass to be in the range $920 \leq M(\pi^+\pi^-\eta) \leq 980 \text{ MeV}/c^2$, which corresponds, approximately, to the range $[-10, +6]\sigma$ of the Gaussian resolution, after performing a kinematic fit constraining the reconstructed mass of the η candidate to the nominal η mass [12]. To identify charged pion candidates, the ratios of PID likelihoods, $R_{i/\pi} = \mathcal{L}_i/(\mathcal{L}_\pi + \mathcal{L}_i)$, are used, where L_π is the likelihood for the track being a pion, while L_i is the corresponding likelihood for the kaon ($i = K$) or electron ($i = e$) hypotheses. We require $R_{K/\pi} \leq 0.6$ and $R_{e/\pi} \leq 0.95$ for pion candidates. The likelihood for each particle species is obtained by combining information from CDC, TOF and ACC [13], and (for electrons only) ECL [14]. According to MC studies, these requirements reject 28% of background, while the resulting efficiency loss is below 3%. Charged pion tracks are required to originate from near the interaction point (IP) by restricting their distance of closest approach to the z axis to be less than 4.0 cm along the z axis and 0.3 cm perpendicular to it, respectively. The z axis is opposite to the direction of the e^+ beam. These selection criteria suppress beam-related backgrounds and reject poorly reconstructed tracks. To reduce systematic uncertainties associated with track reconstruction efficiency, the transverse momenta of charged pions are required to be greater than $100 \text{ MeV}/c$.

To identify $B_s^0 \rightarrow \eta'\eta$ candidates we use (shown here in natural units) the beam-energy-constrained B_s^0 mass, $M_{\text{bc}} = \sqrt{E_{\text{beam}}^2 - p_{B_s}^2}$, the energy difference, $\Delta E = E_{B_s} - E_{\text{beam}}$, and the reconstructed invariant mass of the η' , where E_{beam} , p_{B_s} and E_{B_s} are the beam energy, the momentum and energy of the B_s^0 candidate, respectively. All these quantities are calculated in the e^+e^- center-of-mass frame. To improve the ΔE resolution, the η' candidates are further constrained to the nominal mass of η' , though most of the improvement comes from the η mass constraint. Signal candidates are required to satisfy selection criteria $M_{\text{bc}} > 5.3 \text{ GeV}/c^2$ and $-0.4 \leq \Delta E \leq 0.3 \text{ GeV}$. In a Gaussian approximation, the ΔE resolution is approximately 40 MeV. Similarly, the M_{bc} resolution is $4 \text{ MeV}/c^2$. To take advantage of all available information in case the data indicate signal presence, we include $M(\pi^+\pi^-\eta)$ in the three-dimensional (3D) ML fit used to statistically separate the signal from background. We define the signal region: $5.35 < M_{\text{bc}} < 5.43 \text{ GeV}/c^2$, $-0.25 < \Delta E < 0.10 \text{ GeV}$, and $0.94 < M(\pi^+\pi^-\eta) < 0.97 \text{ GeV}/c^2$. The area outside the signal region is considered as sideband. To optimize sensitivity we use a narrower signal region $5.39 < M_{\text{bc}} <$

$5.43 \text{ GeV}/c^2$ which would contain the largest signal contribution.

Hadronic continuum events from $e^+e^- \rightarrow q\bar{q}$ ($q = u, d, c, s$) are the primary source of background. Because of large initial momenta of the light quarks, continuum events exhibit a ‘‘jetlike’’ event shape, while $B_s^{(*)0}\bar{B}_s^{(*)0}$ events are distributed isotropically. We utilize modified Fox-Wolfram moments [15], used to describe the event topology, to discriminate between signal and continuum background. A likelihood ratio (\mathcal{LR}) is calculated using Fisher discriminant coefficients obtained in an optimization based on these moments. We suppress the background using a discovery-optimized selection on \mathcal{LR} obtained by maximizing the value of Punzi’s figure of merit [16]:

$$\text{FOM} = \frac{\varepsilon(t)}{a/2 + \sqrt{B(t)}}, \quad (1)$$

where t is the requirement on \mathcal{LR} , ε and B are the signal reconstruction efficiency and the number of background events expected in the signal region for a given value of t , respectively. The quantity a is the desired significance (which we vary between 3 and 5) in the units of standard deviation. To predict $B(t)$ we multiply the number of events in the data sideband by the ratio of the numbers of events in the signal region and sideband in the background MC sample. We require signal candidates to satisfy the requirement $\mathcal{LR} \geq 0.95$, which corresponds to $B(0.95) = 3.3$ and 48 background events in the signal region and sideband, respectively. This 47%-efficient requirement removes 99% of background. Using MC simulation we estimate continuum background to comprise 97% of the remaining events.

The background events containing real η' mesons exhibit a peak in the $M(\pi^+\pi^-\eta)$ distribution, however, they are distributed smoothly in M_{bc} and ΔE . The fraction of this peaking background is a free parameter in our ML fits.

About 14% of the reconstructed signal MC events contain multiple candidates primarily arising due to misreconstructed η mesons. In such events we retain the candidate with the smallest value of $\sum \chi_\eta^2 + \chi_{\pi^+\pi^-}^2$, where χ_η^2 denotes the η mass-constrained fit statistic, the summation is over the two η candidates, and $\chi_{\pi^+\pi^-}^2$ quantifies the quality of the vertex fit for two pion tracks. Simulation shows that this procedure selects the correct B_s^0 candidate in 62% of such events. The overall reconstruction efficiency is 10%.

To extract the signal yield, we perform an unbinned extended ML fit to the 3D distribution of M_{bc} , ΔE , and $M(\pi^+\pi^-\eta)$. The likelihood function is

$$\mathcal{L} = \frac{e^{-\sum_j n_j}}{N!} \prod_{i=1}^N \left(\sum_j^3 n_j \mathcal{P}_j[M_{\text{bc}}^i, \Delta E^i, M^i(\pi^+\pi^-\eta)] \right), \quad (2)$$

where i is the event index, N is the total number of events, j denotes the fit component (the three components are background, correctly reconstructed signal, and misreconstructed signal described later), and the parameters n_j represent signal and background yields. Due to negligible correlations among fit variables for both background and correctly reconstructed signal events, the probability density function (PDF) for each fit component is assumed to factorize as $\mathcal{P}[M_{\text{bc}}^i, \Delta E^i, M^i(\pi^+\pi^-\eta)] = \mathcal{P}[M_{\text{bc}}^i] \cdot \mathcal{P}[\Delta E^i] \cdot \mathcal{P}[M^i(\pi^+\pi^-\eta)]$. The signal PDF is represented by a weighted sum of the three PDFs describing possible $B_s^0 \rightarrow \eta'\eta$ signal contributions from $B_s^{(*)0} \bar{B}_s^{(*)0}$ pairs, where the weights are fixed according to previous measurements [11].

To validate our fitting model and adjust the PDF shape parameters used to describe the signal, we use the control sample of $B^0 \rightarrow \eta'K_S^0$ decays. We reconstruct K_S^0 candidates via secondary vertices associated with pairs of oppositely charged pions [17] using a neural network technique [18]. The following information is used in the network: the momentum of the K_S^0 candidate in the laboratory frame; the distance along the z axis between the two track helices at the point of their closest approach; the flight length in the $x-y$ plane; the angle between the K_S^0 momentum and the vector joining the K_S^0 decay vertex to the IP; the angle between the pion momentum and the laboratory-frame K_S^0 momentum in the K_S^0 rest frame; the distance-of-closest-approach in the $x-y$ plane between the IP and the two pion helices; and the pion hit information in the SVD and CDC. The selection efficiency is 87% over the momentum range of interest. We also require that the reconstructed $\pi^+\pi^-$ invariant mass is within $12 \text{ MeV}/c^2$, which is about 3.5σ , of the nominal K_S^0 mass [12]. We require $5.20 \leq M_{\text{bc}} \leq 5.30 \text{ GeV}/c^2$ for B^0 candidates. The control-sample signal region is $5.27 < M_{\text{bc}} < 5.29 \text{ GeV}/c^2$, $-0.20 < \Delta E < 0.10 \text{ GeV}$, and $0.94 < M(\pi^+\pi^-\eta) < 0.97 \text{ GeV}/c^2$. All other selection criteria are the same as those used to select B_s^0 candidates. This control sample is used to validate the η and η' reconstruction and its effect on the resolution functions and PDF shape parameters. The validation of K_S^0 reconstruction was performed previously in a similar B_s^0 analysis [19].

The presence of four photons in the final state gives rise to a sizable misreconstruction probability for the signal events. We study these self-crossfeed (SCF) events using the signal MC sample. A large correlation between M_{bc} and ΔE for such signal events is taken into account by describing the correctly reconstructed signal and SCF

components separately with two different PDF sets. The latter comprise approximately 14% of the reconstructed signal and are excluded from the estimate of its efficiency. The Pearson correlation coefficient for the region with largest correlations for SCF signal events is 27%.

A sum of a Gaussian and a Crystal Ball [20] function is used to model the correctly reconstructed signal in each of the three fit variables. For M_{bc} and $M(\pi^+\pi^-\eta)$ we use a sum of these two functions with the same mean but different widths, while for ΔE both the mean and width are different. A Bukin function [21] and an asymmetric Gaussian are used to model the SCF contribution in M_{bc} and ΔE , respectively. For $M(\pi^+\pi^-\eta)$, we use a sum of a Gaussian and a first-order Chebyshev polynomial. In our nominal fit to data the fraction of correctly reconstructed signal is fixed to its MC value. The signal PDF shape parameters for M_{bc} and ΔE are validated using the $B^0 \rightarrow \eta'K_S^0$ control sample.

We use an ARGUS [22] function to describe the background distribution in M_{bc} and a first-order Chebyshev polynomial for ΔE . To model the peaking part in $M(\pi^+\pi^-\eta)$ we use the signal PDF, because the peak is due to real η' mesons, while an additional first-order Chebyshev polynomial is used for the non-peaking contribution. The projections of the fit to the $B^0 \rightarrow \eta'K_S^0$ control sample are shown in Fig. 1.

To further test and validate our fitting model, ensemble tests are carried out by generating MC pseudoexperiments. In these experiments we use PDFs obtained from full detector simulation and the $B^0 \rightarrow \eta'K_S^0$ data. We perform 1000 pseudoexperiments for each assumed number of signal events. An ML fit is executed for each sample prepared in these experiments. The signal yield distribution obtained from these fits exhibits good linearity. We use the results of pseudoexperiments to construct classical confidence intervals (without ordering) using a procedure due to Neyman [23]. For each ensemble of pseudoexperiments, the lower and upper ends of the respective confidence interval represent the values of fit signal yields for which 10% of the results lie below and above these values, respectively. These intervals are then combined to prepare a classical confidence belt [24, 25] used to make a statistical interpretation of the results obtained from data. The confidence intervals prepared using this statistical method are known to slightly “overcover” for the number of signal events [26], therefore resulting in a conservative upper limit.

We apply the 3D model to the data and obtain 2.7 ± 2.5 signal and 57.3 ± 7.8 background events. The signal-region projections of the fit are shown in Fig. 2. We observe no significant signal and estimate a 90% confidence-level (CL) upper limit on the branching fraction for the decay $B_s^0 \rightarrow \eta'\eta$ using the following formula:

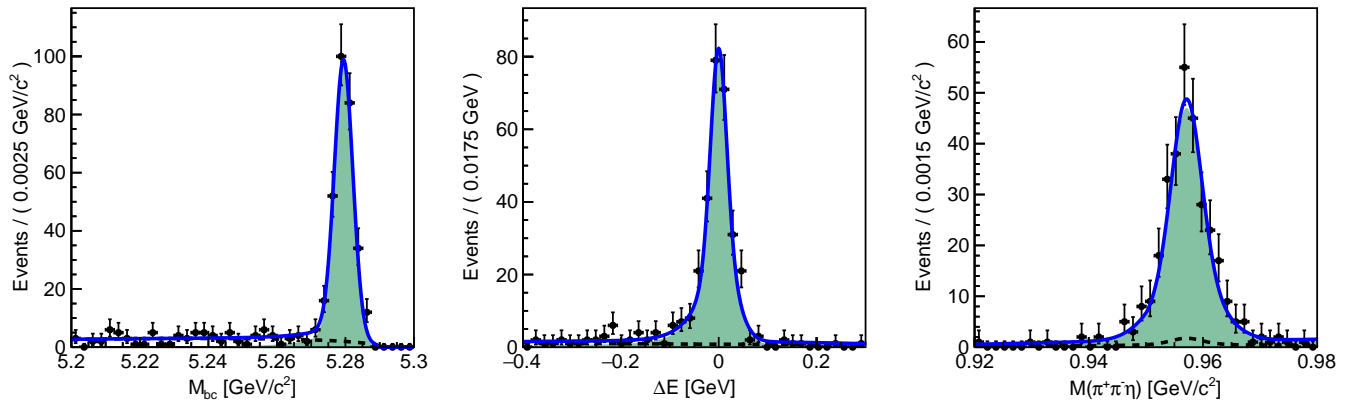


FIG. 1: Signal-region projections of the fit results on M_{bc} , ΔE , and $M(\pi^+\pi^-\eta)$ for the $B^0 \rightarrow \eta'K_S^0$ control sample. Points with error bars are data, blue solid curves are the results of the fit, black dashed curves are the background component, and cyan-filled regions show the signal component.

$$\mathcal{B}(B_s^0 \rightarrow \eta'\eta) < \frac{N_{\text{UL}}^{90\%}}{N_{B_s^0} \times \varepsilon \times \mathcal{B}}, \quad (3)$$

where $N_{B_s^0}$ is the number of B_s^0 mesons in the full Belle data sample, ε is the overall reconstruction efficiency for the signal B_s^0 decay, and \mathcal{B} is the product of the sub-decay branching fractions for η and η' reconstructed in our analysis. Further, $N_{\text{UL}}^{90\%}$ is the expected signal yield of approximately 6.6 events at 90% CL obtained from the confidence belt constructed using the frequentist approach [23]. Using Eq. (3) we estimate a 90% CL upper limit on the branching fraction $\mathcal{B}(B_s^0 \rightarrow \eta'\eta) < 6.2 \times 10^{-5}$. We also estimate a 90% CL upper limit on the product $f_s \times \mathcal{B}(B_s^0 \rightarrow \eta'\eta) < 1.2 \times 10^{-5}$. The systematic uncertainties are not included in these estimates.

Sources of systematic uncertainties and their relative contributions are listed in Table I. The relative uncertainties on f_s and $\sigma(\Upsilon(5S))$ are 15.4% and 4.7%, respectively. The systematic uncertainty due to η reconstruction is 2.1% per η candidate [27]. Track reconstruction [28] and PID systematic uncertainties are 0.35% and 2% per track, respectively. We estimate the systematic uncertainty due to the \mathcal{LR} requirement to be 10%, which represents the relative change in efficiency when this requirement is varied by ± 0.02 about the nominal value of 0.95. This range of variation is defined by the statistics of the control sample which is used to validate the efficiency and its dependence on the \mathcal{LR} requirement. Systematic uncertainty due to signal PDF shape is estimated by varying the fixed parameters within their statistical uncertainties determined with $B^0 \rightarrow \eta'K_S^0$ data. When varying these parameters, we observe an 11% change in the signal yield obtained from the data and use this number as an estimate of PDF parametrization systematics. Systematic

uncertainty due to $f_{B_s^{(*)0}\overline{B}_s^{(*)0}}$ is evaluated by varying relative fractions of possible contributions to signal PDF and is 1.3%. When varying the SCF contribution by $\pm 50\%$ of itself, we observe a 4% change in the results of the fit to data, which we use as an estimate of SCF PDF systematic uncertainty. The relative uncertainties on η and η' branching fractions are 1% and 1.2%, respectively. The statistical uncertainty due to MC statistics is estimated to be 0.1%. The overall systematic uncertainties for $\mathcal{B}(B_s^0 \rightarrow \eta'\eta)$ and $f_s \times \mathcal{B}(B_s^0 \rightarrow \eta'\eta)$ are estimated by adding the individual contributions in quadrature and are 23.1% and 17.2%, respectively. These systematic uncertainties are included in the $N_{\text{UL}}^{90\%}$ estimates of approximately 7.0 and 6.9 events by smearing the fit yield distributions while constructing the confidence belt used to extract the results. We estimate the upper limits on the branching fraction $\mathcal{B}(B_s^0 \rightarrow \eta'\eta) < 6.5 \times 10^{-5}$ and on the product $f_s \times \mathcal{B}(B_s^0 \rightarrow \eta'\eta) < 1.3 \times 10^{-5}$ at 90% CL. Finally, using the number of signal events obtained from the fit we estimate $\mathcal{B}(B_s^0 \rightarrow \eta'\eta) = (2.5 \pm 2.2 \pm 0.6) \times 10^{-5}$ and $f_s \times \mathcal{B}(B_s^0 \rightarrow \eta'\eta) = (0.51 \pm 0.44 \pm 0.09) \times 10^{-5}$, where, for each of the two estimates, the first uncertainty is statistical and the second is systematic. We summarize the results in Table II.

In summary, we have used the full data sample recorded by the Belle experiment at the $\Upsilon(5S)$ resonance to search for the decay $B_s^0 \rightarrow \eta'\eta$. We observe no statistically significant signal and set a 90% CL upper limit of 6.5×10^{-5} on its branching fraction. To date, our result is the only experimental information on $B_s^0 \rightarrow \eta'\eta$ and is twice as large as the most optimistic SM-based theoretical prediction. This decay can be probed further at the next-generation Belle II experiment [29] at the SuperKEKB collider in Japan.

We thank the KEKB group for the excellent operation of the accelerator; the KEK cryogenics group

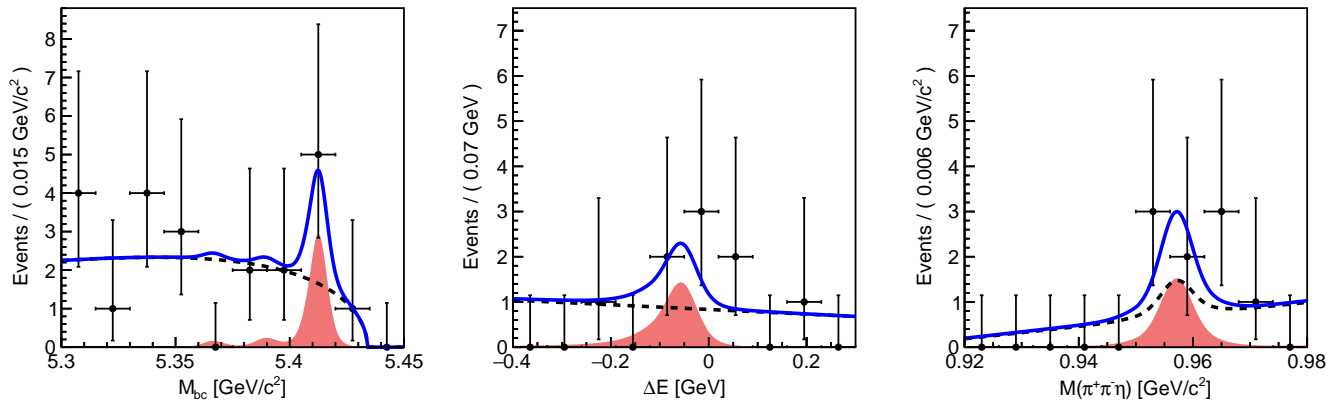


FIG. 2: Signal-region projections of the fit results on M_{bc} , ΔE , and $M(\pi^+\pi^-\eta)$ for $B_s^0 \rightarrow \eta'\eta$. The M_{bc} signal region of the dominant signal contribution, $5.39 < M_{bc} < 5.43$ GeV/c^2 , is used to plot the ΔE and $M(\pi^+\pi^-\eta)$ projections. Points with error bars are the results of the fit, black dashed curves are the background component, and pink-filled regions show the signal component.

TABLE I: Summary of systematic uncertainties.

Source	Uncertainty (%)
f_s	15.4
$\sigma(\Upsilon(5S))$	4.7
η reconstruction	4.2
Tracking	0.7
PID	4.0
\mathcal{LR} selection	10.0
PDF parametrization	11.0
$f_{B_s^{(*)0}\bar{B}_s^{(*)0}}$	1.3
SCF PDF	4.0
Branching fraction of η	1.0
Branching fraction of η'	1.2
MC statistics	0.1

TABLE II: Summary of the results for $f_s \times \mathcal{B}(B_s^0 \rightarrow \eta'\eta)$ and $\mathcal{B}(B_s^0 \rightarrow \eta'\eta)$. See the text for more information.

Quantity	Value
$f_s \times \mathcal{B}(B_s^0 \rightarrow \eta'\eta)$	$(0.51 \pm 0.44 \pm 0.09) \times 10^{-5}$ $< 1.3 \times 10^{-5}$ @ 90% CL
$\mathcal{B}(B_s^0 \rightarrow \eta'\eta)$	$(2.5 \pm 2.2 \pm 0.6) \times 10^{-5}$ $< 6.5 \times 10^{-5}$ @ 90% CL

for the efficient operation of the solenoid; and the KEK computer group, and the Pacific Northwest National Laboratory (PNNL) Environmental Molecular Sciences Laboratory (EMSL) computing group for strong computing support; and the National Institute of Informatics, and Science Information NETWORK 5 (SINET5) for valuable network support. We acknowledge support from the Ministry of Education, Culture, Sports, Science, and Technology (MEXT) of Japan, the Japan Society for the Promotion of Science (JSPS), and the Tau-Lepton Physics Research Center of Nagoya University; the Australian Research Council including grants DP180102629, DP170102389, DP170102204, DP150103061, FT130100303; Austrian Federal Ministry of Education, Science and Research (FWF) and FWF Austrian Science Fund No. P 31361-N36; the National Natural Science Foundation of China under Contracts No. 11435013, No. 11475187, No. 11521505, No. 11575017, No. 11675166, No. 11705209; Key Research Program of Frontier Sciences, Chinese Academy of Sciences (CAS), Grant No. QYZDJ-SSW-SLH011; the CAS Center for Excellence in Particle Physics (CCEPP); the Shanghai Pujiang Program under Grant No. 18PJ1401000; the Shanghai Science and Technology Committee (STCSM) under Grant No. 19ZR1403000; the Ministry of Education, Youth and Sports of the Czech Republic under Contract No. LTT17020; Horizon 2020 ERC Advanced Grant No. 884719 and ERC Starting Grant No. 947006 “InterLeptons” (European Union); the Carl Zeiss Foundation, the Deutsche Forschungsgemeinschaft, the Excellence Cluster Universe, and the VolkswagenStiftung; the Department of Atomic Energy (Project Identification No. RTI 4002) and the Department of Science and Technology of India; the Istituto Nazionale di Fisica Nucleare of Italy; National Research

Foundation (NRF) of Korea Grant Nos. 2016R1D1A1B-01010135, 2016R1D1A1B02012900, 2018R1A2B3003643, 2018R1A6A1A06024970, 2018R1D1A1B07047294, 2019K1A3A7A09033840, 2019R1I1A3A01058933; Radiation Science Research Institute, Foreign Large-size Research Facility Application Supporting project, the Global Science Experimental Data Hub Center of the Korea Institute of Science and Technology Information and KREONET/GLORIAD; the Polish Ministry of Science and Higher Education and the National Science Center; the Ministry of Science and Higher Education of the Russian Federation, Agreement 14.W03.31.0026, and the HSE University Basic Research Program, Moscow; University of Tabuk research grants S-1440-0321, S-0256-1438, and S-0280-1439 (Saudi Arabia); the Slovenian Research Agency Grant Nos. J1-9124 and P1-0135; Ikerbasque, Basque Foundation for Science, Spain; the Swiss National Science Foundation; the Ministry of Education and the Ministry of Science and Technology of Taiwan; and the United States Department of Energy and the National Science Foundation.

-
- [1] Ed. A. J. Bevan, B. Golob, Th. Mannel, S. Prell, and B. D. Yabsley, *Eur. Phys. J. C* **74**, 3026 (2014); SLAC-PUB-15968; KEK Preprint 2014-3.
- [2] E. Kou *et al.*, *Prog. Theor. Exp. Phys.* **2019**, 123C01 (2019).
- [3] Y.-K. Hsiao, C.-F. Chang, and X.-G. He, *Phys. Rev. D* **93**, 114002 (2016).
- [4] A. R. Williamson and J. Zupan, *Phys. Rev. D* **74**, 014003 (2006).
- [5] A. Ali *et al.*, *Phys. Rev. D* **76**, 074018 (2007).
- [6] H.-Y. Cheng and C.-K. Chua, *Phys. Rev. D* **80**, 114026 (2009).
- [7] H.-Y. Cheng, C.-W. Chiang, and A.-L. Kuo, *Phys. Rev. D* **91**, 014011 (2015).
- [8] R. Aaij *et al.* (LHCb Collaboration), *Phys. Rev. Lett.* **115**, 051801 (2015).
- [9] S. Kurokawa and E. Kikutani, *Nucl. Instrum. Methods Phys. Res. Sect. A* **499**, 1 (2003), and other papers included in this Volume; T. Abe *et al.*, *Prog. Theor. Exp. Phys.* **2013**, 03A001 (2013) and references therein.
- [10] A. Abashian *et al.* (Belle Collaboration), *Nucl. Instrum. Methods Phys. Res. Sect. A* **479**, 117 (2002); also see Section 2 in J. Brodzicka *et al.*, *Prog. Theor. Exp. Phys.* **2012**, 04D001 (2012).
- [11] S. Esen *et al.* (Belle Collaboration), *Phys. Rev. D* **87**, 031101(R) (2013).
- [12] P.A. Zyla *et al.* (Particle Data Group), *Prog. Theor. Exp. Phys.* **2020**, 083C01 (2020).
- [13] E. Nakano, *Nucl. Instrum. Methods Phys. Res. Sect. A* **494**, 402 (2002).
- [14] K. Hanagaki, H. Kakuno, H. Ikeda, T. Iijima and T. Tsukamoto, *Nucl. Instrum. Methods Phys. Res. Sect. A* **485**, 490 (2002).
- [15] The Fox-Wolfram moments were introduced in G. C. Fox and S. Wolfram, *Phys. Rev. Lett.* **41**, 1581 (1978). The Fisher discriminant used by Belle, based on modified Fox-Wolfram moments, is described in K. Abe *et al.* (Belle Collaboration), *Phys. Rev. Lett.* **87**, 101801 (2001) and K. Abe *et al.* (Belle Collaboration.), *Phys. Lett. B* **511**, 151 (2001).
- [16] G. Punzi, eConf C **030908** (2003), arXiv:physics/0308063 [physics.data-an].
- [17] H. Nakano, SEARCH FOR NEW PHYSICS BY A TIME-DEPENDENT CP VIOLATION ANALYSIS OF THE DECAY $B \rightarrow K_S \eta \gamma$ USING THE BELLE DETECTOR. PhD Thesis, Tohoku University (2014) Chapter 4, unpublished.
- [18] M. Feindt and U. Kerzel, *Nucl. Instrum. Methods Phys. Res. Sect. A* **559**, 190 (2006).
- [19] B. Pal *et al.* (Belle Collaboration), *Phys. Rev. Lett.* **116**, 161801 (2016).
- [20] M. Oreglia, A STUDY OF THE REACTIONS $\psi' \rightarrow \gamma \gamma \psi$. PhD thesis, SLAC-0236, 1980; T. Skwarnicki, A STUDY OF THE RADIATIVE CASCADE TRANSITIONS BETWEEN THE UPSILON-PRIME AND UPSILON RESONANCES. PhD thesis, DESY-F31-86-02, 1986.
- [21] A.D. Bukin, arXiv:0711.4449 [physics.data-an] (2007).
- [22] H. Albrecht *et al.* (ARGUS Collaboration), *Phys. Lett. B* **241**, 278-282 (1990).
- [23] J. Neyman, *Phil. Trans. Roy. Soc. Lond. A* **236**, 767, 333-380 (1937); Reprinted in *A Selection of Early Statistical Papers of J. Neyman*, (University of California Press, Berkeley, 1967).
- [24] A. Stuart and J.K. Ord, *Classical Inference and Relationship*, 5th ed., Kendall's Advanced Theory of Statistics, Vol. 2 (Oxford University Press, New York, 1991); see also earlier editions by Kendall and Stuart.
- [25] W.T. Eadie, D. Drijard, F.E. James, M. Roos, and B. Sadoulet, *Statistical Methods in Experimental Physics*, (NorthHolland, Amsterdam, 1971).
- [26] G. J. Feldman and R. D. Cousins, *Phys. Rev. D* **57**, 3873-3889 (1998).
- [27] J. Schumann *et al.* (Belle Collaboration), *Phys. Rev. Lett.* **97**, 061802 (2006).
- [28] S. Ryu *et al.* (Belle Collaboration), *Phys. Rev. D* **89**, 072009 (2014).
- [29] T. Abe *et al.* (Belle II Collaboration), arXiv: 1011.0352 [physics.ins-det] (2010).